JEBAT, 2023, Vol 6, No 1, 34-43
https://doi.org/10.54987/jebat.v6i1.813

JOURNAL OF ENVIRONMENTAL BIOREMEDIATION AND TOXICOLOGY
Website: http://journal.hibiscuspublisher.com/index.php/JEBAT/index

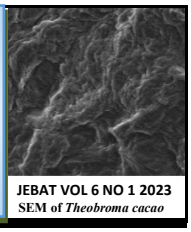

Biosorption of Zn (II) onto Rice Husk Ash: Isothermal Remodelling

Bilal Ibrahim Dan-Iya[1], Mohd Ezuan Khayat[1] and Mohd Yunus Shukor[1]*

[1]Department of Biochemistry, Faculty of Biotechnology and Biomolecular Sciences, Universiti Putra Malaysia, 43400 UPM Serdang, Selangor, Malaysia.

*Corresponding author:
Mohd Yunus Shukor,
Department of Biochemistry,
Faculty of Biotechnology and Biomolecular Sciences,
Universiti Putra Malaysia,
43400 UPM Serdang,
Selangor, Malaysia.
Email: hmyakasai.bch@buk.edu.ng

HISTORY

Received: 5th March 2023
Received in revised form: 23rd June 2023
Accepted: 25th July 2023

KEYWORDS

Rice husks ash
Zinc
Biosorption
Isotherm
Freundlich

ABSTRACT

Zn is a heavy metal often found at elevated concentrations in effluents as high as 300 ppm from the rubber processing industry as it is used for the vulcanization of rubber. The rice milling process produces rice husk as a by-product. It is one of the most important agricultural leftovers in terms of volume. The data of the sorption isotherm of Zn (II) (CV) sorption onto rice husk ash, which was plotted using linearized plots of isothermal models were reanalyzed using isothermal models using nonlinear regression. As the datapoints were small, isotherms with parameters of only up to three were utilized to prevent overfitting. The nineteen models were Henry, Langmuir, Freundlich, Temkin, Dubinin-Radushkevich, Jovanovic, Redlich-Peterson, Sips, Toth, Hill, Khan, BET, Vieth-Sladek, Radke-Prausnitz, Brouers–Sotolongo, Fritz-Schlunder III, Unilan, Fowler-Guggenheim and Moreau. Statistical analysis based on error function analyses such as root-mean-square error (RMSE), adjusted coefficient of determination (adjR^2), accuracy factor (AF), bias factor (BF), Bayesian Information Criterion (BIC), corrected AICc (Akaike Information Criterion), and Hannan-Quinn Criterion (HQC) showed that Freundlich, followed by Langmuir and the Jovanovic models as the best top three models. The value of the maximum monolayer adsorption capacity for Zn binding to rice husk ash according to the Langmuir's parameter q_{mL} was 7.33 mg g-1 (95% Confidence interval from5.464 to 9.187), while b_L (L mg^{-1}), the Langmuir model constants was 0.011 L mg^{-1} (95% C.I. from 0.030 to 0.182). As the Freundlich equation is unable to model the maximum adsorption, the Halsey rearrangement of the Freundlich equation was utilized and gave the estimated maximum absorption of 7.20 mg g^{-1}, which is very close to the experimental value. The constant values obtained in this study, especially the Langmuir model are largely different from the previously reported linearized approach.

INTRODUCTION

Rubber exports brought in between one and two billion dollars a year for Malaysia. Even while the expansion of the rubber goods manufacturing sector in Malaysia has been good for the country's economy, the industry's heavy water consumption and the environmental harm it has caused are two sides of the same coin. Malaysia's economy has benefited from the growth of the rubber goods manufacturing industry [1–3]. It is stated that the manufacture of rubber thread contributes the most to the pollution problem among the industries dealing with rubber goods. The main concern is the alarmingly high concentration of zinc in the effluent. About 135 organizations fall within this category (latex products, tires and tubes, industrial and general rubber goods, and footwear). The wastewater produced by these companies has a high concentration of organic waste, as measured by the chemical oxygen demand (COD) and biological oxygen demand (BOD). The abundance of organic debris in the sewer water lends credence to these conclusions [4–7]. The department of environment in Malaysia has defined guidelines for the pH of wastewater, and this value is significantly lower than the permissible value range.

Furthermore, it was found that the levels of pollutants in this wastewater were the highest compared to the levels of contaminants found in wastewater from facilities producing other types of rubber goods. Many different methods, such as activated sludge or anaerobic digestion, aerated lagoons, anaerobic/facultative ponding, and so on, are used in the last stage of wastewater treatment in the rubber products manufacturing business. Flocculation is a common step in the pretreatment process for removing zinc from wastewater but is

expected to become an expensive method in the years to come [8–12]. Some of the new and improved treatment procedures that have been developed as a result of this issue are currently making their way to facilities of this type. Many various treatment processes have been proposed in the literature as viable options for extracting heavy metals including zinc from water supplies. These include coagulation, chemical precipitation, evaporation, electrolysis, adsorption, and reverse osmosis. However, these older forms of technology may not be enough, may be too costly, or may introduce new complications. Therefore, adsorption is likely the most appealing of these approaches since it is easy to apply and competitive and effective [13–19]. But the cost of the adsorbent and the energy needed for its replenishment might act as a roadblock to future progress.

The reuse and/or recycling of garbage and other similar materials is becoming an increasingly important topic, and there is a corresponding increase in interest in the use of inexpensive materials for adsorptive uses. One area where this is becoming increasingly important is in the field of adsorptive materials, where both the need for and demand in inexpensive options is expanding. Several recent studies have described research that makes use of adsorbents such rice husk and ash, which are cheap and readily available in the area where the research was conducted [20–24].

Biosorption is a method for decontaminating dirty water that does not involve any danger and is very cost effective. Biosorbents may be made from either biomass or natural substrates. In recent years, a great deal of research on mercury biosorption that is of a high quality and was conducted at a reasonable cost has been published. Adsorbents that can be acquired in vast numbers with little to no effort, that are prevalent in the natural world, or that are by-products of industrial processes are examples of low-cost adsorbents. Rice husk may be used as a fuel to create steam, which allows a variety of enterprises to cut their costs for both energy and materials. Rice husk ash is the ash that is left over after burning rice husk and is collected in a dust collector that is positioned upstream from the stacks of rice husk-fired boilers and furnaces. This gives the ash its name (RHA). RHA has been utilized in the past to successfully do this task because to the powerful adsorption qualities that it possesses [20–24].

It is absolutely necessary to have an accurate assignment of the kinetics and isotherms of the biosorption process in order to have an adequate understanding of the biosorption process in these species. A linearized form of what is plainly a nonlinear curve of these data is commonly reported in the scientific literature. When nonlinear data is linearized, the error structure of the data is changed. This makes it more difficult to quantify uncertainty, which is sometimes portrayed as a confidence range of 95 percent. The aim of this work is to remodel a published work on Zn sorption to rice husk ash [25], which utilize linear regression to obtain best fitting models.

METHOD

Data acquisition and fitting

Figure 2 data from a previously published study [25] was digitized using the freeware Webplotdigitizer 2.5 [26]. After that, the data were nonlinearly regressed using the curve-fitting program Curve-Expert Professional (Version 2.6.5, copyright Daniel Hyams). Implicit equations were solved using MATLAB (Mathworks, Massachusetts, United States). Digitization using this program has been praised for its dependability [27].

Isotherms

As the value of the datapoints is very small, only models having parameters of up to three were considered to prevent overfitting.

Table 1. Mathematical models that were used in modelling data [28,29].

Isotherm	*p*	Formula	Ref.
Henry's law	1	$q_e = HC_e$	[30]
Langmuir	2	$q_e = \frac{q_{mL} b_L C_e}{1 + b_L C_e}$	[28]
Jovanovic	2	$q_e = q_{mJ}(1 - e^{-K_J C_e})$	[31]
Freundlich	2	$q_e = K_F C_e^{\frac{1}{n_F}}$	[32]
Dubinin-Radushkevich	2	$q_e = q_{mDR} exp\left\{-K_{DR}\left[RTln\left(1 + \frac{1}{C_e}\right)\right]^2\right\}$	[33,34]
Temkin	3	$q_e = \frac{RT}{b_T}\{ln(a_T C_e)\}$	[35,36]
Redlich-Peterson	3	$q_e = \frac{K_{RP1} C_e}{1 + K_{RP2} C_e^{\beta_{RP}}}$	[37]
Sips	3	$q_e = \frac{K_s q_{mS} C_e^{\frac{1}{n_S}}}{1 + K_s C_e^{\frac{1}{n_S}}}$	[38]
Toth	3	$q_e = \frac{q_{mT} C_e}{\left(K_T + C_e^{n_T}\right)^{n_T}}$	[39]
Hill	3	$q_e = \frac{q_{mH} C_e^{n_H}}{K_H + C_e^{n_H}}$	[40]
Khan	3	$q_e = \frac{q_{mK} b_K C_e}{(1 + b_K C_e)^{a_K}}$	[41]
BET	3	$q_e = \frac{q_{mBET} \alpha_{BET} C_e}{(1 - \beta_{BET} C_e)(1 - \beta_{BET} C_e + \alpha_{BET} C_e)}$	[42]
Vieth-Sladek	3	$q_e = \frac{q_{mVS} b_{VS} C_e}{(1 + b_{VS} C_e)^{n_{VS}}}$	[43]
Radke-Prausnitz	3	$q_e = \frac{q_{mRP} K_{RP} C_e}{(1 + K_{RP} C_e)^{n_{RP}}}$	[44]
Brouers–Sotolongo	3	$q_e = q_{mBS}\left(1 - \exp\left(-K_{BS} C_e^{\frac{1}{n_{BS}}}\right)\right)$	[45]
Fritz-Schlunder-III	3	$q_e = \frac{q_{mFS} K_{FS} C_e}{1 + K_{FS} C_e^{n_{FS}}}$	[46]
Fowler-Guggenheim*	3	$q_e = q_{mFG} \frac{K_L C_e e^{\frac{\alpha q_e}{q_{mFG}}}}{1 + K_L C_e e^{\frac{\alpha q_e}{q_{mFG}}}}$	[47]
Moreau	3	$q_e = q_{mM} \frac{bC_e + lb^2 {C_e}^2}{1 + 2bC_e + lb^2 {C_e}^2}$	[48]
Unilan	3	$q_e = \frac{q_{mU}}{2b_U} ln\left(\frac{a_U + C_e e^{b_U}}{a_U + C_e e^{-b_U}}\right)$	

Note *Implicit equation or function.

Statistical analysis

A set of statistical discriminatory tests were utilized to find the best model and are as follows;

The RMSE was computed using Equation 1, and it stands to reason that the fewer parameters utilized, the smaller the RMSE will be. n is for the total number of observations made in the experiment, Obi and Pdi stand for the total number of observations made in the experiment and projections, and p stands for the total number of parameters [49] .

$$RMSE = \sqrt{\frac{\sum_{i=1}^{n}(Pd_i - Ob_i)^2}{n-p}} \qquad \text{(Eqn. 1)}$$

Because R^2 or the coefficient of determination ignores the number of parameters in a model, the modified R^2 is used to overcome this limitation. The entire variance of the y-variable is given by S^2_y in the equation (**Equations 2** and **3**), while RMS is the Residual Mean Square.

$$Bias\ factor = 10\left(\sum_{i=1}^{n} log\frac{(Pd_i/Ob_i)}{n}\right) \qquad \text{(Eqn. 2)}$$

$$Accuracy\ factor = 10\left(\sum_{i=1}^{n} log\frac{|(Pd_i/Ob_i)|}{n}\right) \quad \text{(Eqn. 3)}$$

The AICc is computed as follows (**Equation 4**), where p represents the number of parameters and n represents the number of data points. The corrected Akaike information criterion (AICc) is used to manage data with a large number of parameters but a limited number of values [50]. A model with a lower AICc score is considered more likely to be right [50]. The information theory is the foundation of the Akaike Information Criterion (AIC). It strikes a compromise between the goodness of fit of a given model and the model's complexity [51].

$$AICc = 2p + n\ln\left(\frac{RSS}{n}\right) + \frac{2(p+1)+2(p+2)}{n-p-2} \quad \text{(Eqn. 4)}$$

Another statistical tool based on information theory apart from AICc, is the Bayesian Information Criterion (BIC) (Equation 5). The number of parameters is penalized more severely by this error function than by AIC [26].

$$BIC = n\ln\left(\frac{RSS}{n}\right) + k\ln(n) \quad \text{(Eqn. 5)}$$

The Hannan-Quinn information criterion (HQC) (**Equation 6**) is another error function approach based on information theory. Because of the ln ln n element in the calculation, the HQC is more consistent than the AIC [50].

$$HQC = nIn\left(\frac{RSS}{n}\right) + 2k\ln(\ln n) \quad \text{(Eqn. 6)}$$

The Accuracy Factor (AF) and Bias Factor (BF) are two further error function analyses derived from Ross's work [50]. These error functions evaluate models statistically for goodness-of-fit but do not penalize for the number of parameters (**Equations 7** and **8**).

$$Adjusted\ (R^2) = 1 - \frac{RMS}{S_Y^2} \quad \text{(Eqn. 7)}$$

$$Adjusted\ (R^2) = 1 - \frac{(1-R^2)(n-1)}{(n-p-1)} \quad \text{(Eqn. 8)}$$

Marquardt's percent standard deviation (MPSD) is another penalty-imposed error function that has been extensively utilized in numerous isotherm studies. The function has some similarity to a geometric mean error distribution that is altered according to the system's number of degrees of freedom [52]. Among the first to use this error function in the adsorption field is [53] and the error function's official term that is known as MPSD (Equation 9) was introduced by the McKay group [54].

$$MPSD = 100\sqrt{\frac{1}{n-p}\sum_{i=1}^{n}\left(\frac{Ob_i - Pd_i}{Ob_i}\right)^2} \quad \text{(Eqn. 9)}$$

where n is the number of experimental data, p is the number of parameters, Ob_i is the experimental data, and Pd_i is the value predicted by the model.

RESULTS AND DISCUSSION

The equilibrium data from [55] was analyzed using the models—Henry, Langmuir, Freundlich, Redlich-Petersen, Sips, BET, Toth, Hill, Khan, Vieth-Sladek, Radke-Prausnitz, Unilan, Fritz-Schlunder III, Fritz-Schlunder IV, and Fritz-Schlunder V, were used in finding the best fit by utilizing non-linear regression. Henry, Langmuir, Hill, Vieth-Sladek, Unilan, Sips and BET does not fit well with the data, whereas Freundlich, Redlich-Petersen, Toth, Khan, Radke-Prausnitz, Fritz-Schlunder III, Fritz-Schlunder IV, and Fritz-Schlunder V, fitted well with the data (**Figs. 1 – 19**). The best isotherm model was found to be the Freundlich with the best combination of low values for AICc, BIC, HQC and RMSE and values of AF, BF and adjR^2 values closest to unity. This is followed (descending order) by Langmuir and Jovanovic as the next top three best model (**Table 2**). As enough models fitted well with the charred rice husk data, it explains and justifies the more accuracy of using nonlinear regression as against the linear regression used in the original publication which suggests the 2-parameter Jovanovic isotherm as the best model.

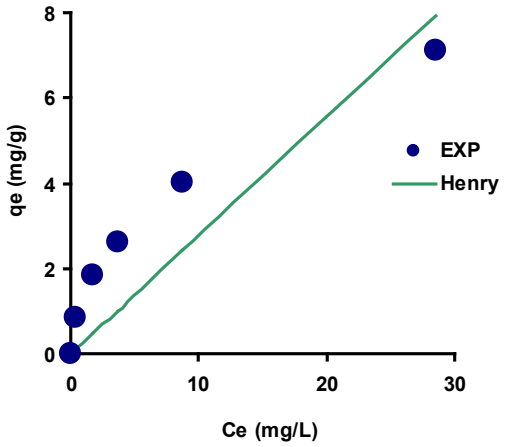

Fig. 1. Adsorption isotherm of Zn (II) onto rice husk ash as modelled using the Henry model.

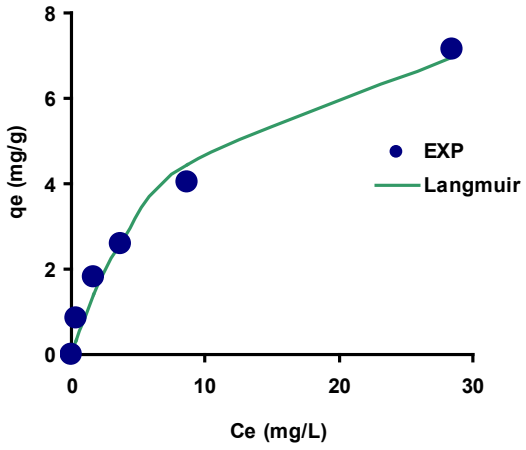

Fig. 2. Adsorption isotherm of Zn (II) onto rice husk ash as modelled using the Langmuir isotherm model.

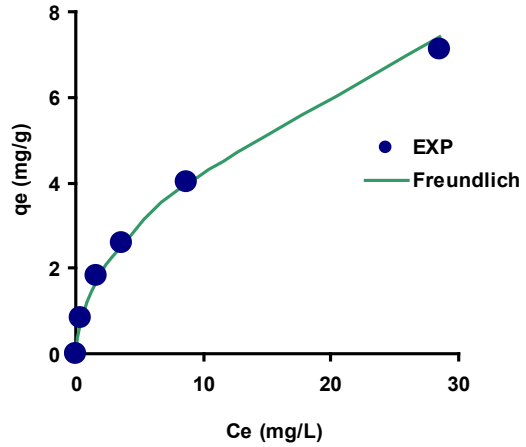

Fig. 3. Adsorption isotherm of Zn (II) onto rice husk ash as modelled using the Freundlich isotherm model.

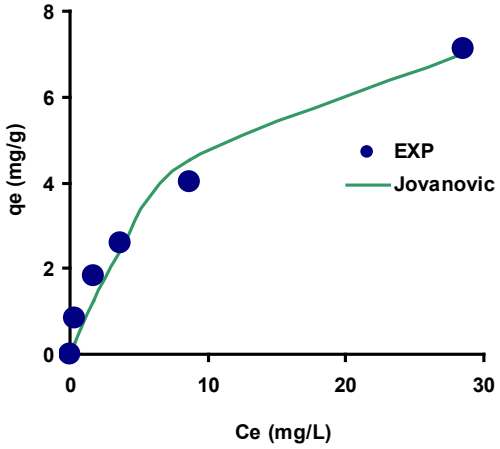

Fig. 6. Adsorption isotherm of Zn (II) onto rice husk ash as modelled using the Jovanovic isotherm model.

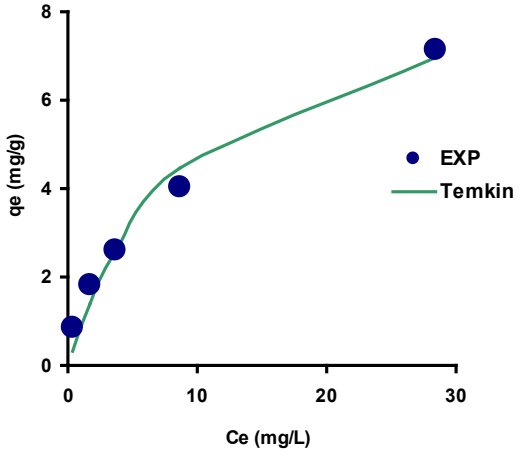

Fig. 4. Adsorption isotherm of Zn (II) onto rice husk ash as modelled using the Temkin isotherm model.

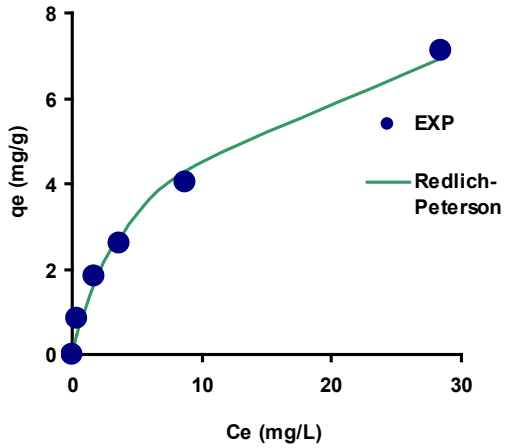

Fig. 7. Adsorption isotherm of Zn (II) onto rice husk ash as modelled using the Redlich-Peterson isotherm model.

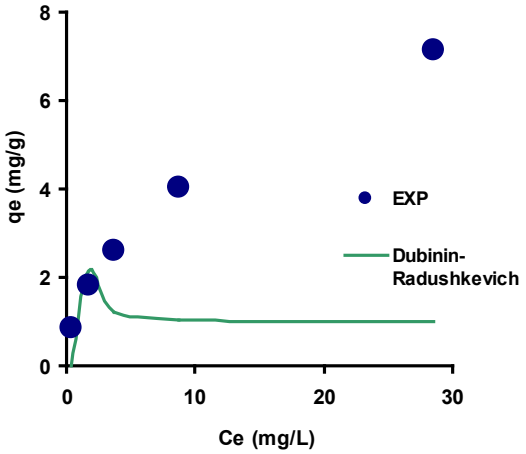

Fig. 5. Adsorption isotherm of Zn (II) onto rice husk ash as modelled using the Dubinin-Radushkevich isotherm model.

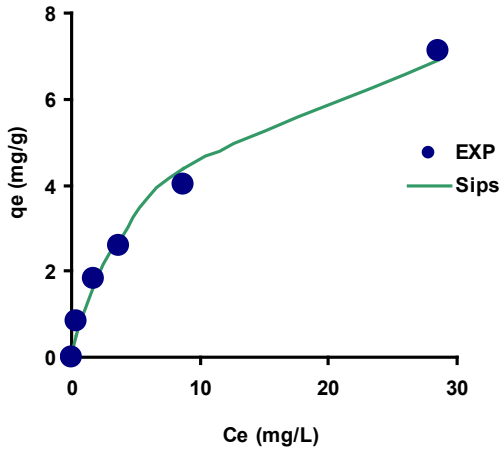

Fig. 8. Adsorption isotherm of Zn (II) onto rice husk ash as modelled using the Sips isotherm model.

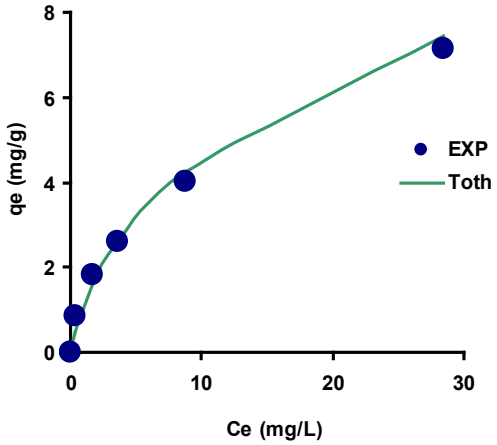

Fig. 9. Adsorption isotherm of Zn (II) onto rice husk ash as modelled using the Toth isotherm model.

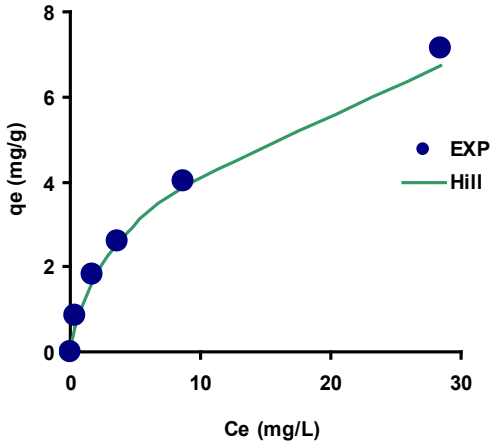

Fig. 10. Adsorption isotherm of Zn (II) onto rice husk ash as modelled using the Hill isotherm model.

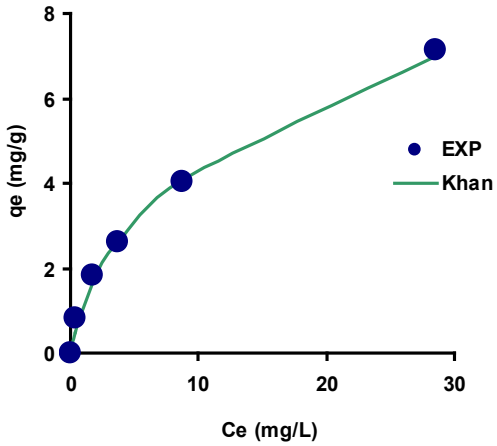

Fig. 11. Adsorption isotherm of Zn (II) onto rice husk ash as modelled using the Khan isotherm model.

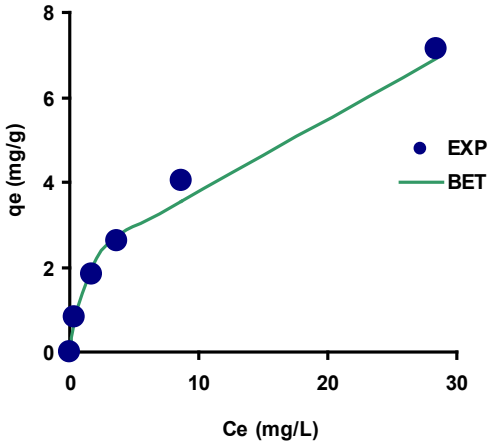

Fig. 12. Adsorption isotherm of Zn (II) onto rice husk ash as modelled using the BET isotherm model.

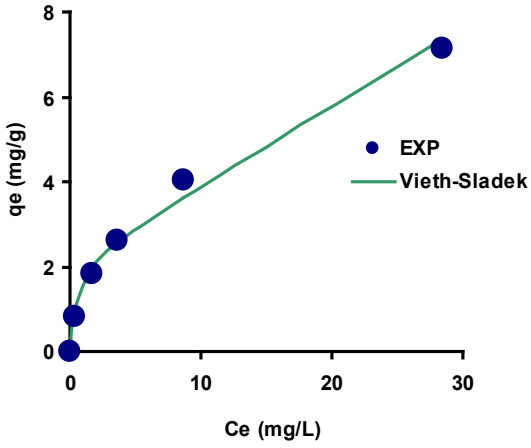

Fig. 13. Adsorption isotherm of Zn (II) onto rice husk ash as modelled using the Vieth-Sladek isotherm model.

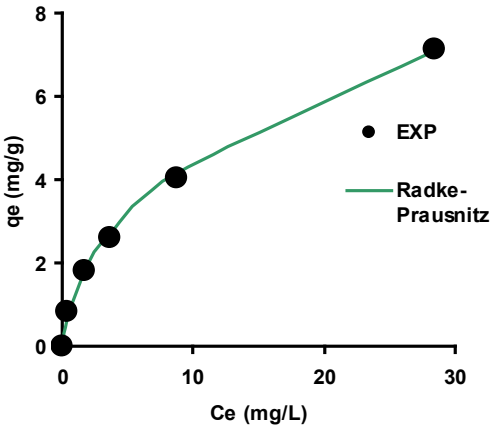

Fig. 14. Adsorption isotherm of Zn (II) onto rice husk ash as modelled using the Radke-Prausnitz isotherm model.

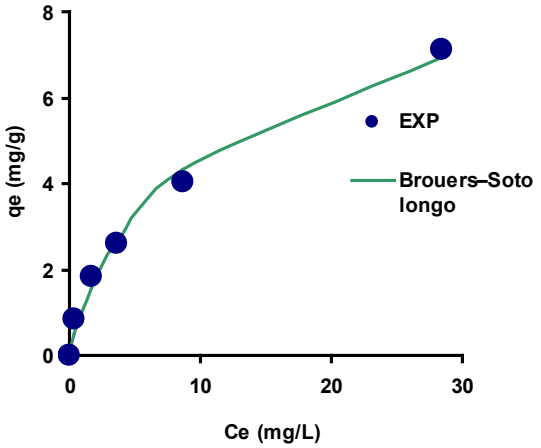

Fig. 15. Adsorption isotherm of Zn (II) onto rice husk ash as modelled using the Brouers-Sotolongo isotherm model.

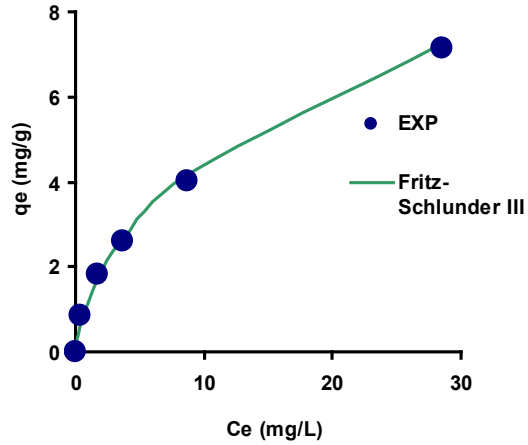

Fig. 16. Adsorption isotherm of Zn (II) onto rice husk ash as modelled using the Fritz-Schlunder III isotherm model.

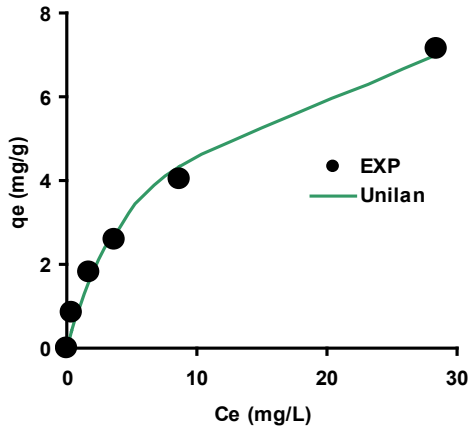

Fig. 17. Adsorption isotherm of Zn (II) onto rice husk ash as modelled using the Unilan isotherm model.

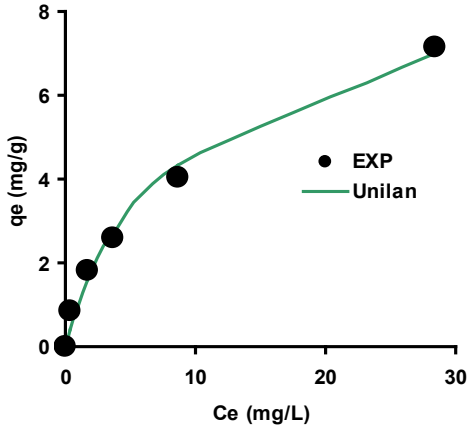

Fig. 18. Adsorption isotherm of Zn (II) onto rice husk ash as modelled using the Fowler Guggenheim isotherm model.

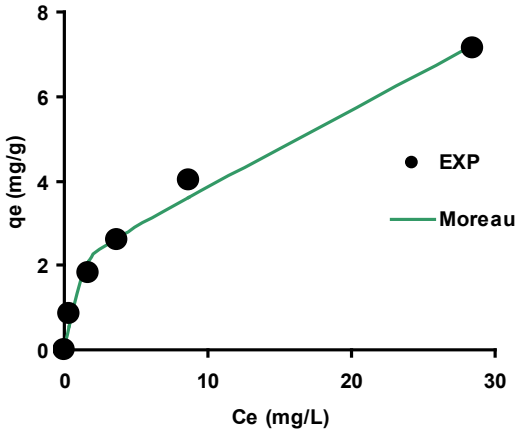

Fig. 19. Adsorption isotherm of Zn (II) onto rice husk ash as modelled using the Moreau isotherm model.

Table 2. Error function analysis for the fitting of the isotherm of Zn (II) onto rice husk ash.

Model	p	RMSE	adR^2	AICc	BIC	HQC	BF	AF
Freundlich	2	0.17	0.99	-1.85	-9.65	-21.52	0.97	1.05
Langmuir	2	0.41	0.97	8.77	3.64	-10.90	0.83	1.25
Jovanovic	2	0.49	0.96	11.09	16.21	-8.57	0.78	1.34
Henry	1	1.28	0.78	11.85	0.00	3.02	0.44	2.34
Radke-Prausnitz	3	0.14	1.00	26.32	-12.70	-24.18	0.97	1.06
Fritz-Schlunder III	3	0.18	0.993	28.97	-12.39	-21.53	0.95	1.07
Khan	3	0.24	0.99	32.77	-13.12	-17.73	0.90	1.12
Dubinin-Radushkevich	2	3.51	-24.04	34.62	-7.85	14.95	0.25	4.23
Hill	3	0.30	0.98	35.50	-12.28	-15.00	0.91	1.10
Redlich-Peterson	3	0.30	0.98	35.56	-7.32	-14.94	0.91	1.14
Vieth-Sladek	3	0.31	0.98	35.92	-12.12	-14.58	1.03	1.08
Brouers–Sotolongo	3	0.32	0.98	36.23	-22.31	-14.27	0.91	1.14
Toth	3	0.32	0.98	36.34	-12.27	-14.16	0.90	1.14
Sips	3	0.32	0.98	36.35	-13.06	-14.15	0.92	1.13
Moreau	3	0.33	0.98	36.38	-1.81	-14.12	0.94	0.94
BET	3	0.33	0.97	36.51	-15.85	-13.99	0.97	1.07
Unilan	3	0.35	0.97	37.09	-19.65	-13.41	0.88	1.17
Temkin	3	0.47	0.95	40.77	-20.26	-9.73	0.83	1.25
Fowler-Guggenheim	3	0.78	0.85	46.82	-11.54	-3.68	0.92	0.92

Note:
RMSE Root mean Square Error
adR^2 Adjusted Coefficient of determination
p no of parameters
AF Accuracy factor
BF Bias factor
BIC Bayesian Information Criterion
AICc Adjusted Akaike Information Criterion
HQC Hannan–Quinn information criterion

Langmuir isotherm

The Langmuir isotherm is one of several isotherm models that are mechanistic rather than empirical. The model envisioned adsorbate being adsorbed onto the adsorbent in a single, uniform layer. For monolayer adsorption to take place, the isotherm assumes that all adsorption sites have the same energy and that the adsorbent is structurally homogenous [56]. Due to the exponential reduction of intermolecular interactions with increasing distance, this isotherm model predicts the occurrence of monolayer coverage of the adsorbent at the outer surface of the adsorbent. In addition to simplifying the linear relationship, this model predicts a constant monolayer adsorption capacity. The model also predicts that the Henry's model become valid for both very dilute and very concentrated solute concentrations [57].

The Langmuir, together with the Freundlich model are amongst the most utilized models and appear in nearly all sorption works. The maximum adsorption parameter and the model constant predicted using the nonlinear regression approach was nearly the same to the original study but could not provide the 95% confidence interval for the estimated parameters. The value of the maximum monolayer adsorption capacity for Zn binding to rice husk ash according to the Langmuir's parameter q_{mL} was 7.33 mg g-1 (95% Confidence interval from5.464 to 9.187), while b_L (L mg^{-1}), the Langmuir model constants was 0.011 L mg^{-1} (95% C.I. from 0.030 to 0.182). These values are much lower than the reported linear regressed values in the original publication [25]. Literature search showed that biosorption of Zinc (II) using microbial and plant-based adsorbents exhibits a maximum adsorption capacity of between 5 and 50 mg g^{-1}. Only activated carbon-based adsorbent exceeds 100 mg g^{-1} (**Table 3**), which is a typical result.

Freundlich isotherm

One common empirical model for adsorption and desorption is the Freundlich equation, which was first derived for the gas phase. The adsorbate creates a monomolecular layer on the adsorbent's surface in a Freundlich adsorption isotherm. While the Freundlich equation does give some useful empirical data on particle sorption, its applicability is limited at a particular concentration, at which point it becomes nonlinear [58–60]. Unlike the Langmuir isotherm, the Freundlich model can be generalized to multilayer adsorption. This isotherm model allows for a heterogeneous surface to have a variable distribution of adsorption heat and affinities. The model also proposed an exponential distribution of the active sites and energy for adsorbate binding and also presumes surface heterogeneity. The Freundlich isotherm model was first used to describe the adsorption of an adsorbate onto charcoal.

The mass ratio of the adsorbate onto the adsorbent changed as the concentration of the solution changed. This means that the sum of the adsorption at each site is equal to the adsorbed amount. Once the most stable binding sites are occupied, the adsorption energy drops at an exponential rate [57,61,62]. The Freundlich model was also the best model for Zn sorption to Streptomyces sp. [19], leaves of *Corchorus olitorius* [63], activated carbon/silica compo-site [64] and to coffee waste [65] (**Table 3**).

In other examples, the Freundlich model was also the best model for lead(II) sorption by a modified Jordanian zeolite [66], by a Guar gum/bentonite bionanocomposite [67], *Chlorococcum aquaticum* biomass [68] and nanoparticle adsorbents of cellulose origin [69] and the sorption of other metal and radionuclides [70–75].

Because of its empirical nature, the Freundlich model is unable to forecast the maximal adsorption capacity in which K_F ((mg g^{-1}.L mg^{-1})$^{1/nF}$) is the Freundlich isotherm constant, and n_F is the Freundlich exponent. A small $1/n_F$ value indicates a heterogenous system [58,76]. Since there is only a single KF term in the Freundlich equation, this shows that the adsorption energy on a homogeneous surface is unaffected by the quantity of surface coverage. Various slopes in Freundlich isotherms are often seen as evidence of multiple binding sites, and researchers have drawn many inferences regarding adsorption processes based on the KF and 1/nF parameters. These inferences, however, are very speculative, and the KF and 1/nF parameters should not be used as a basis for them [77]. As the Freundlich equation is unable to model the maximum adsorption, the Halsey rearrangement of the Freundlich equation [78] (**Equation 10**) gave the estimated maximum absorption of 7.20 mg g^{-1}, which is very close to the experimental value.

$$K_F = \frac{q_{mF}}{c_e^{\frac{1}{n_F}}} \qquad \text{(Eqn. 10)}$$

Jovanovic isotherm

The Jovanovic isotherm is similar to the Langmuir in that it takes into account an adsorption surface assumption. In this case, we can use a second approximation for monolayer adsorption that accounts for the lack of lateral interactions. The surface binding vibrations of an adsorbed species are taken into account, which is the main difference between this model and the Langmuir model [31]. The isotherm also takes into account the adsorbed species' surface binding vibrations. Multilayer adsorption can also be accounted for with the help of a 3-parameter Jovanovic isotherm [31].

Table 3. Summary of recent Zn (II) sorption studies.

Adsorbent	Kinetics	Isotherm	Linear or Nonlinear Regression	Experimental uptake, Q_e (mg/g)	Reference
Streptomyces sp.	PSO	Freundlich	L	4.65	[19]
Saccharomyces cerevisiae	PSO	Dubinin–Radushkevich	L	20.38	[79]
Sargassum polycystum,	PSO	Langmuir	NL	116.2	[80]
Alium Cepa seed biomass	PSO	Langmuir	NL	1.68	[81]
alginate extraction process waste	PSO		NL	51.06	[14]
leaves of *Corchorus olitorius*	n.a.	Freundlich	L	11.63 (Langmuir)	[63]
Sulfuric acid treated-sugarcane bagasse	PSO	Langmuir	L	1.292	[82]
Activated carbon/silica composite	n.a.	Freundlich	L	344.82 (Langmuir)	[64]
NaOH-treated rice husk	PSO	Langmuir	L	20.08	[83]
Scenedesmus sp. MCC 26	n.a.	Freundlich	L	142.85 (Langmuir)	[84]
Coffee waste	n.a.	Freundlich	L	46.05 (Langmuir)	[65]
oil palm waste ash particles	PFO	Langmuir	NL	10.655	[85]

Table 4. Isothermal models' constants for the top-three models.

Model		Unit	Value	(95% confidence interval)
Freundlich[#]	K_F	(mg g^{-1}.L mg^{-1})$^{1/nF}$	1.41	1.388 to 1.435
	n_F	(L mg^{-1})	2.07	2.043 to 2.092
	q_{mF}	mg g^{-1}	7.20	
Langmuir	q_{mL}	mg g^{-1}	9.3	6.515 to 12.077
	b_L	L mg^{-1}	0.011	0.030 to 0.182
Jovanovic	q_{mJ}	mg g^{-1}	7.33	5.464 to 9.187
	K_J	dimensionless	0.11	0.043 to 0.177

Note
[#]Isotherms that have no direct way in estimating the maximum adsorption capacity (mg g^{-1}).

Metal removal from wastewater can be accomplished using a variety of sorbents prepared by coating, chemical synthesis, and other methods [18,86–97]. Rice husk is a waste product created during the milling of rice. In terms of total volume, it is among the most significant agricultural byproducts. It's responsible for about 20% of the total rice output in some nations [98,99]. It is estimated that developing countries would produce 500 million tons of rice each year, with around 100 million tons of rice husk available for utilization. Historically, rice husks have been employed not only by the rice industry as a fuel source for boilers, but also in the production of blocks used in civil construction as panels [99,100]. However, there are many more rice husks available that can be used locally, leading to disposal problems. The granular structure, chemical stability, and inexpensive production costs of this material led to its selection, as did the fact that it does not require regeneration.

CONCLUSION

Finally, multiple models with one to three parameters have been fitted using non-linear regression to the adsorption isotherm data of Zn (II) dye onto rice husk ash. Root-mean-square error (RMSE), adjusted coefficient of determination ($adjR^2$), bias factor (BF), accuracy factor (AF), bias information coefficient (BIC), and the corrected Akaike Information Criterion (AICc) all indicate that the showed that the Freundlich model was the best model in terms of overall best criteria. The Freundlich model is unable to forecast the maximal adsorption capacity. The Halsey rearrangement of the Freundlich equation gave the estimated maximum absorption of 7.20 mg g^{-1}, which is very close to the experimental value. The value of the maximum monolayer adsorption capacity for Zn binding to rice husk ash according to the Langmuir's parameter q_{mL} was 7.33 mg g^{-1} (95% Confidence interval from5.464 to 9.187), while b_L (L mg^{-1}), the Langmuir model constants was 0.011 L mg^{-1} (95% C.I. from 0.030 to 0.182). These values are much lower than the reported linear regressed values in the original publication The nonlinear regression approach represents parameter values in the 95% confidence interval range, which allows for better comparison with published findings.

REFERENCE

1. Karthikeyan T, Rajgopal S, Miranda LR. Chromium(VI) adsorption from aqueous solution by Hevea Brasilinesis sawdust activated carbon. J Hazard Mater. 2005;124(1–3):192–9.
2. Gupta VK, Nayak A, Agarwal S, Tyagi I. Potential of activated carbon from waste rubber tire for the adsorption of phenolics: Effect of pre-treatment conditions. J Colloid Interface Sci. 2014;417:420–30.
3. Islam MT, Saenz-Arana R, Hernandez C, Guinto T, Ahsan MA, Bragg DT, et al. Conversion of waste tire rubber into a high-capacity adsorbent for the removal of methylene blue, methyl orange, and tetracycline from water. J Environ Chem Eng. 2018;6(2):3070–82.
4. Mohammadi M, Man HC, Hassan MA, Yee PL. Treatment of wastewater from rubber industry in Malaysia. Afr J Biotechnol. 2010;9(38):6233–43.
5. Edirisinghe JC. Taxing the Pollution: A Case for Reducing the Environmental Impacts of Rubber Production in Sri Lanka. J South Asian Dev. 2014 Apr 1;9(1):71–90.
6. Massoudinejad M, Mehdipour-Rabori M, Hadi Dehghani M. Treatment of natural rubber industry wastewater through a combination of physicochemical and ozonation processes. J Adv Environ Health Res. 2015 Dec 1;3(4):242–9.
7. Ngteni R, Hossain MS, Ab Kadir MO, Asis AJ, Tajudin Z. Kinetics and Isotherm Modeling for the Treatment of Rubber Processing Effluent Using Iron (II) Sulphate Waste as a Coagulant. Water. 2020 Jun;12(6):1747.
8. Somasundaran P, Ren Y, Yelloji Rao M. Applications of biological processes in mineral processing. Colloids Surf Physicochem Eng Asp. 1998;133(1–2):13–23.
9. Myagchenkov VA, Proskurina VE. Kinetics of flocculation and densification in ocher suspension in the presence of polyacrylamide, poly(ethylene oxide), and their 1 : 1 mixture. Colloid J Russ Acad Sci Kolloidn Zhurnal. 2000;62(5):588–93.
10. Zhang CL, Cui YN, Wang Y. Bioflocculant produced from bacteria for decolorization, Cr removal and swine wastewater application. Sustain Environ Res. 2012;22(2):129–34.
11. Ge X, Wu Z, Cravotto G, Manzoli M, Cintas P, Wu Z. Cork wastewater purification in a cooperative flocculation/adsorption process with microwave-regenerated activated carbon. J Hazard Mater. 2018;360:412–9.
12. Usefi S, Asadi-Ghalhari M. Modeling and optimization of the coagulation-flocculation process in turbidity removal from aqueous solutions using rice starch. Pollution. 2019;5(3):623–36.
13. Tarhriz V, Akbari Z, Dilmaghani A, Hamidi A, Hejazi MA, Hejazi MS. Bioreduction of Iron and Biosorption of Heavy Metals (Ni2+, Co2+, Pb2+) by a Novel Environmental Bacterium, Tabrizicola aquatica RCRI19T. Asian J Water Environ Pollut. 2019;16(3):73–81.
14. Cardoso SL, Costa CSD, da Silva MGC, Vieira MGA. Insight into zinc(II) biosorption on alginate extraction residue: Kinetics, isotherm and thermodynamics. J Environ Chem Eng. 2020 Jun 1;8(3):103629.
15. Carvalho JTT, Milani PA, Consonni JL, Labuto G, Carrilho ENVM. Nanomodified sugarcane bagasse biosorbent: synthesis, characterization, and application for Cu(II) removal from aqueous medium. Environ Sci Pollut Res. 2021;28(19):24744–55.
16. Fathollahi A, Khasteganan N, Coupe SJ, Newman AP. A meta-analysis of metal biosorption by suspended bacteria from three phyla. Chemosphere. 2021 Apr 1;268:129290.
17. Cao W, Li H, Hong Y, Yang Z, Fu M. Preparation and Characterization of Spherical Lignocellulose-based Anion Exchanger from Sugarcane Bagasse. BioResources. 2022;17(3):3984–4000.
18. Narayanasamy S, Sundaram V, Sundaram T, Vo DVN. Biosorptive ascendency of plant based biosorbents in removing hexavalent chromium from aqueous solutions – Insights into isotherm and kinetic studies. Environ Res. 2022 Jul 1;210:112902.
19. Kumari S, Agrawal NK, Agarwal A, Kumar A, Malik N, Goyal D, et al. A Prominent Streptomyces sp. Biomass-Based Biosorption of Zinc (II) and Lead (II) from Aqueous Solutions: Isotherm and Kinetic. Separations. 2023 Jul;10(7):393.
20. Mesfin Yeneneh A, Maitra S, Eldemerdash U. Study on biosorption of heavy metals by modified lignocellulosic waste. J Appl Sci. 2011;11(21):3555–62.
21. Yeneneh AM, Thanabalan M, Demerdash UMNE. Biosorption of heavy metals by potassium hydrogen phosphate and sodium oxalate modified lignocellulosic waste. In: 2011 National Postgraduate Conference - Energy and Sustainability: Exploring the Innovative Minds, NPC 2011. 2011.
22. Younis ShA, El-Gendy NSh, El-Azab WI, Moustafa YM, Hashem AI. The biosorption of phenol from petroleum refinery wastewater using spent waste biomass. Energy Sources Part Recovery Util Environ Eff. 2014;36(23):2566–78.
23. Garg R, Garg R, Thakur A, Arif SM. Water remediation using biosorbent obtained from agricultural and fruit waste. Mater Today Proc. 2020;46:6669–72.

24. Jagaba AH, Kutty SRM, Khaw SG, Lai CL, Isa MH, Baloo L, et al. Derived hybrid biosorbent for zinc(II) removal from aqueous solution by continuous-flow activated sludge system. J Water Process Eng. 2020 Apr 1;34:101152.
25. Ag ES, Na B, Se G. Adsorption of Heavy Metal Ions from Aqueous Solutions onto Rice Husk Ash Low Cost Adsorbent. Environ Anal Toxicol. 2018;8(1):1–5.
26. Dan-Iya BI, Shukor MY. Isothermal Modelling of the Adsorption of Chromium onto Calcium Alginate Nanoparticles. J Environ Microbiol Toxicol. 2021;9(2):1–7.
27. Khare KS, Phelan FR. Quantitative Comparison of Atomistic Simulations with Experiment for a Cross-Linked Epoxy: A Specific Volume-Cooling Rate Analysis. Macromolecules. 2018;51(2):564–75.
28. Langmuir I. THE ADSORPTION OF GASES ON PLANE SURFACES OF GLASS, MICA AND PLATINUM. J Am Chem Soc. 1918;40(2):1361–402.
29. Schirmer W. Physical Chemistry of Surfaces. Z Für Phys Chem. 1999;210(1):134–5.
30. Ridha FN, Webley PA. Anomalous Henry's law behavior of nitrogen and carbon dioxide adsorption on alkali-exchanged chabazite zeolites. Sep Purif Technol. 2009;67(3):336–43.
31. Jovanović DS. Physical adsorption of gases - I: Isotherms for monolayer and multilayer adsorption. Kolloid-Z Amp Z Für Polym. 1969;235(1):1203–13.
32. Carmo AM, Hundal LS, Thompson ML. Sorption of hydrophobic organic compounds by soil materials: Application of unit equivalent Freundlich coefficients. Environ Sci Technol. 2000;34(20):4363–9.
33. Radushkevich LV. Potential theory of sorption and structure of carbons. Zhurnal Fiz Khimii. 1949;23:1410–20.
34. Dubinin MM. Modern state of the theory of volume filling of micropore adsorbents during adsorption of gases and steams on carbon adsorbents. Zh Fiz Khim. 1965;39(6):1305–17.
35. Temkin MI, Pyzhev V. Kinetics of ammonia synthesis on promoted iron catalysts. Acta Physicochim USSR. 1940;12(3):327–56.
36. Chu KH. Revisiting the Temkin Isotherm: Dimensional Inconsistency and Approximate Forms. Ind Eng Chem Res [Internet]. 2021 Aug 16 [cited 2022 Sep 1]; Available from: https://pubs.acs.org/doi/pdf/10.1021/acs.iecr.1c01788
37. Redlich O, Peterson DL. A Useful Adsorption Isotherm. Shell Dev Co Emeryv Calif. 1958;63:1024.
38. Sips R. On the structure of a catalyst surface. J Chem Phys. 1948;16(5):490–5.
39. Tóth J. Uniform interpretation of gas/solid adsorption. Adv Colloid Interface Sci. 1995;55(C):1–239.
40. Hill AV. The possible effects of the aggregation of the molecules of haemoglobin on its dissociation curves. J Physiol. 1910;40:iv–vii.
41. Khan AA, Singh RP. Adsorption thermodynamics of carbofuran on Sn (IV) arsenosilicate in H+, Na+ and Ca2+ forms. Colloids Surf. 1987;24(1):33–42.
42. Brunauer S, Emmett PH, Teller E. Adsorption of Gases in Multimolecular Layers. J Am Chem Soc. 1938;60(2):309–19.
43. Vieth WR, Sladek KJ. A model for diffusion in a glassy polymer. J Colloid Sci. 1965;20(9):1014–33.
44. Radke CJ, Prausnitz JM. Adsorption of Organic Solutes from Dilute Aqueous Solution of Activated Carbon. J Am Chem Soc. 1972;11(4):445–51.
45. Hamissa AMB, Brouers F, Mahjoub B, Seffen M. Adsorption of Textile Dyes Using Agave Americana (L.) Fibres: Equilibrium and Kinetics Modelling. Adsorpt Sci Technol. 2007 Jun 1;25(5):311–25.
46. Fritz W, Schluender EU. Simultaneous adsorption equilibria of organic solutes in dilute aqueous solutions on activated carbon. Chem Eng Sci. 1974;29(5):1279–82.
47. Chu KH, Tan B. Is the Frumkin (Fowler–Guggenheim) adsorption isotherm a two- or three-parameter equation? Colloid Interface Sci Commun. 2021 Nov 1;45:100519.
48. Martucci A, Braschi I, Bisio C, Sarti E, Rodeghero E, Bagatin R, et al. Influence of water on the retention of methyl tertiary-butyl ether by high silica ZSM-5 and Y zeolites: A multidisciplinary study on the adsorption from liquid and gas phase. RSC Adv. 2015;5(106):86997–7006.
49. Motulsky HJ, Ransnas LA. Fitting curves to data using nonlinear regression: a practical and nonmathematical review. FASEB J. 1987;1(5):365–74.
50. Burnham KP, Anderson DR. Multimodel inference: Understanding AIC and BIC in model selection. Sociol Methods Res. 2004;33(2):261–304.
51. Akaike H. A New Look at the Statistical Model Identification. IEEE Trans Autom Control. 1974;19(6):716–23.
52. Marquardt DW. An Algorithm for Least-Squares Estimation of Nonlinear Parameters. J Soc Ind Appl Math. 1963;11(2):431–41.
53. Seidel A, Gelbin D. On applying the ideal adsorbed solution theory to multicomponent adsorption equilibria of dissolved organic components on activated carbon. Chem Eng Sci. 1988 Jan 1;43(1):79–88.
54. Porter JF, McKay G, Choy KH. The prediction of sorption from a binary mixture of acidic dyes using single- and mixed-isotherm variants of the ideal adsorbed solute theory. Chem Eng Sci. 1999;54(24):5863–85.
55. Homagai PL, Poudel R, Poudel S, Bhattarai A. Adsorption and removal of crystal violet dye from aqueous solution by modified rice husk. Heliyon. 2022;8(4):e09261.
56. Langmuir I. The constitution and fundamental properties of solids and liquids. Part I. Solids. J Am Chem Soc. 1916;38(11):2221–95.
57. Foo KY, Hameed BH. Insights into the modeling of adsorption isotherm systems. Chem Eng J. 2010;156(1):2–10.
58. Freundlich H. Über die adsorption in lösungen (Over the adsorption in solution). Z Für Phys Chem. 1907;57(1):385–470.
59. Barkhordar B, Ghias Aldin M. Comparision of Langmuir and Freundlich equilibriums in Cr, Cu and Ni adsorption by Sargassum. Iran J Environ Health Sci Eng. 2004 Jan 1;1(2):58–64.
60. Crittenden JC, Watson HM. Adsorption. In: MWH's Water Treatment: Principles and Design, Third Edition [Internet]. John Wiley & Sons, Ltd; 2012 [cited 2020 May 31]. p. 1117–262. Available from: https://onlinelibrary.wiley.com/doi/abs/10.1002/9781118131473.ch15
61. Al-Ghouti MA, Da'ana DA. Guidelines for the use and interpretation of adsorption isotherm models: A review. J Hazard Mater. 2020 Jul 5;393:122383.
62. Hu Q, Pang S, Wang D. In-depth Insights into Mathematical Characteristics, Selection Criteria and Common Mistakes of Adsorption Kinetic Models: A Critical Review. Sep Purif Rev. 2021 Jul 1;0(0):1–19.
63. Ali MM, Bhakta JN. Biosorption of zinc from aqueous solution using leaves of Corchorus olitorius as a low-cost biosorbent. Water Environ Res. 2020;92(6):821–8.
64. Karnib M, Kabbani A, Holail H, Olama Z. Heavy Metals Removal Using Activated Carbon, Silica and Silica Activated Carbon Composite. Energy Procedia. 2014 Dec 31;50:113–20.
65. Kumaraswamy K, Dhananjaneyulu BV, Vijetha P, Siva Jagadish Kumar M. Removal of zinc from aqueous solution using coffee industry waste. Int J Pharma Bio Sci. 2014;5(1):B201–9.
66. Baker H. Removal of Lead Ions from Waste Water Using Modified Jordanian Zeolite. Chem Sci Int J. 2020 Nov 9;19–30.
67. Ahmad R, Mirza A. Synthesis of Guar gum/bentonite a novel bionanocomposite: Isotherms, kinetics and thermodynamic studies for the removal of Pb (II) and crystal violet dye. J Mol Liq. 2018 Jan 1;249:805–14.
68. Liyanage LMM, Lakmali WGM, Athukorala SNP, Jayasundera KB. Application of live Chlorococcum aquaticum biomass for the removal of Pb(II) from aqueous solutions. J Appl Phycol. 2020 Dec 1;32(6):4069–80.
69. Yakubu A, Olatunji GA, Adekola FA. Modified/Unmodified Nanoparticle Adsorbents of Cellulose Origin With High Adsorptive Potential for Removal of Pb(II) From Aqueous Solution. Eur Sci J ESJ. 2017 Sep 30;13(27):425–425.
70. Daifullah A a. M, Moloukhia H. Removal of cobalt and europium radioisotopes using activated carbon prepared from apricot stones. Isot Radiat Res [Internet]. 2002 Jul 1 [cited 2022 Jul 26];34. Available from: https://www.osti.gov/etdeweb/biblio/20395653
71. Moloukhia H, El-Zakla T, Belacy N. Use of lignocellulosic biomass in removal of 60 Co and 13'4 Cs from radioactive wastewater. Arab J Nucl Sci Appl. 2010;43(1):121–30.
72. Rajapaksha AU, Vithanage M, Jayarathna L, Kumara CK. Natural Red Earth as a low cost material for arsenic removal: Kinetics and

the effect of competing ions. Appl Geochem. 2011 Apr 1;26(4):648–54.
73. Mahapatra A, Mishra BG, Hota G. Electrospun Fe2O3–Al2O3 nanocomposite fibers as efficient adsorbent for removal of heavy metal ions from aqueous solution. J Hazard Mater. 2013 Aug 15;258–259:116–23.
74. Sharifi S, Nabizadeh R, Akbarpour B, Azari A, Ghaffari HR, Nazmara S, et al. Modeling and optimizing parameters affecting hexavalent chromium adsorption from aqueous solutions using Ti-XAD7 nanocomposite: RSM-CCD approach, kinetic, and isotherm studies. J Environ Health Sci Eng. 2019 Dec 1;17(2):873–88.
75. Calderón C, Levío-Raimán M, Diez MC. Cadmium removal for marine food application: comparative study of different adsorbents. Int J Environ Sci Technol [Internet]. 2021 Oct 29 [cited 2022 Jul 26]; Available from: https://doi.org/10.1007/s13762-021-03746-9
76. Rushton G, Karns C, Shimizu K. A critical examination of the use of the Freundlich isotherm in characterizing molecularly imprinted polymers (MIPs). Anal Chim Acta. 2005 Jan 3;528:107–13.
77. Sparks DL, Singh B, Siebecker MG. Environmental Soil Chemistry, Third Edition [Internet]. Academic Press; 2023 [cited 2023 Aug 28]. Available from: https://scholars.ttu.edu/en/publications/environmental-soil-chemistry-third-edition
78. Hamdaoui O, Naffrechoux E. Modeling of adsorption isotherms of phenol and chlorophenols onto granular activated carbon: Part I. Two-parameter models and equations allowing determination of thermodynamic parameters. J Hazard Mater. 2007 Aug 17;147(1):381–94.
79. Savastru E, Bulgariu D, Zamfir CI, Bulgariu L. Application of Saccharomyces cerevisiae in the Biosorption of Co(II), Zn(II) and Cu(II) Ions from Aqueous Media. Water. 2022 Jan;14(6):976.
80. Jayakumar V, Govindaradjane S, Rajamohan N, Rajasimman M. Biosorption potential of brown algae, Sargassum polycystum, for the removal of toxic metals, cadmium and zinc. Environ Sci Pollut Res. 2022 Jun 1;29(28):41909–22.
81. Sheikh Z, Amin M, Khan N, Khan MN, Sami SK, Khan SB, et al. Potential application of Allium Cepa seeds as a novel biosorbent for efficient biosorption of heavy metals ions from aqueous solution. Chemosphere. 2021 Sep 1;279:130545.
82. Al-Saidi HM, Gahlan AA, Farghaly OA. Decontamination of Zinc, Lead and Nickel from Aqueous Media by Untreated and Chemically Treated Sugarcane Bagasse: A Comparative Study. Egypt J Chem. 2022;65(3):711–20.
83. Zhang Y, Zheng R, Zhao J, Zhang Y, Wong P keung, Ma F. Biosorption of Zinc from Aqueous Solution Using Chemically Treated Rice Husk. BioMed Res Int. 2013 Jun 11;2013:e365163.
84. Sarwa P, Verma S. Recovery and Recycling of Zn(II) from Wastewater by Scenedesmus sp. MCC 26 Isolated from a Heavy Metal Contaminated Site. CLEAN - Soil Air Water. 2014 Sep 1;42.
85. Chu KH, Hashim MA. Adsorption and desorption characteristics of zinc on ash particles derived from oil palm waste. J Chem Technol Biotechnol. 2002;77(6):685–93.
86. Abbas M, Cherfi A, Kaddour S, Aksil T. Adsorption in simple batch experiments of Coomassie blue G-250 by apricot stone activated carbon - Kinetics and isotherms modeling. Desalination Water Treat. 2015 Jul 14;57:1–12.
87. Tomul F, Arslan Y, Kabak B, Trak D, Kendüzler E, Lima EC, et al. Peanut shells-derived biochars prepared from different carbonization processes: Comparison of characterization and mechanism of naproxen adsorption in water. Sci Total Environ. 2020 Jul 15;726:137828.
88. Adenan NH, Lim YY, Ting ASY. Nocardiopsis sp. for the Removal of Triphenylmethane Dyes: Decolorization and Optimization Studies. Water Air Soil Pollut. 2021;232(10).
89. Crespão LP, Rosenberger AG, Lima FDS, Delgado Bertéli MB, Dragunski DC, Colauto NB, et al. Sugarcane biomass colonized by Pleurotus ostreatus for red 4B dye removal: a sustainable alternative. Environ Technol U K. 2021;42(17):2611–23.
90. Jofre FM, Hernández-Pérez AF, Santos JCD, Felipe MDGDA. Use of dry yeast biomass as a new approach for detoxification of hemicellulosic hydrolysates aiming to xylitol production. Ind Crops Prod. 2021;170.
91. Mallakpour S, Tabesh F. Green and plant-based adsorbent from tragacanth gum and carboxyl-functionalized carbon nanotube hydrogel bionanocomposite for the super removal of methylene blue dye. Int J Biol Macromol. 2021 Jan 1;166:722–9.
92. Yusnimar, Sasmita D, Fadli A. Determination of Pb(II) ion Adsorption Isotherm Model by Regenerated Spent Bleaching Earth (RSBE). J Phys Conf Ser. 2021 Oct;2049(1):012015.
93. Homagai PL, Bhattarai M, Radhika KM, Ghimire KN, Paudyal H, Bhattarai A. Comparative study of Hg(ii) biosorption performance of xanthated and charred sugarcane bagasse from aqueous solutions. RSC Adv. 2022;12(46):29865–77.
94. Ravindiran G, Gaddam K, Sunil K. Experimental Investigation on Reactive Orange 16 Removal Using Waste Biomass of *Ulva prolifera*. Adv Mater Sci Eng. 2022 May 23;2022:e7323588.
95. Zhou X, Maimaitiniyazi R, Wang Y. Some consideration triggered by misquotation of Temkin model and the derivation of its correct form. Arab J Chem. 2022 Nov 1;15(11):104267.
96. Al-Qodah Z, Dweiri R, Khader M, Al-Sabbagh S, Al-Shannag M, Qasrawi S, et al. Processing and characterization of magnetic composites of activated carbon, fly ash, and beach sand as adsorbents for Cr(VI) removal. Case Stud Chem Environ Eng. 2023 Jun 1;7:100333.
97. Ma M, Wang R, Xu M. Thorium(IV) triggers ferroptosis through disrupting iron homeostasis and heme metabolism in the liver following oral ingestion. J Hazard Mater. 2023 Jun 15;452:131217.
98. Daifullah AAM, Girgis BS, Gad HMH. Utilization of agro-residues (rice husk) in small waste water treatment plans. Mater Lett. 2003;57(11):1723–31.
99. Abdelwahab O, Nemr A El, El-Sikaily A, Khaled A. Use of rice husk for adsorption of direct dyes from aqueous solution: A case study of direct F. Scarlet Green synthesis of TiO2 nanoparticles and its toxicity View project Industrial valorization of local biological materials and wastes for wastewater tre. Egypt J Aquat Res. 2005;31(May).
100. Della VP, Kühn I, Hotza D. Caracterização de cinza de casca de arroz para uso como matéria-prima na fabricação de refratários de sílica. Quimica Nova. 2001;24(6):778–82.